Coherence function control of Quantum Dot Superluminescent Light Emitting Diodes by frequency selective optical feedback

Martin Blazek[1,*], **Wolfgang Elsäßer**[1], **Mark Hopkinson**[2], **Patrick Resneau**[3], **Michel Krakowski**[3], **Mattia Rossetti**[4], **Paolo Bardella**[4], **Mariangela Gioannini**[4] **and Ivo Montrosset**[4]

[1]*Institute of Applied Physics, Darmstadt University, Schloßgartenstr. 7, D-64289 Darmstadt, Germany*
[2]*Electronic and Electrical Engineering, University of Sheffield, Mappin Street, Sheffield, S1 3JD, United Kingdom*
[3]*Alcatel Thales, III-V Lab, Route départementale 128, 91767 Palaiseau, France*
[4]*Dipartimento di Elettronica, Politecnico di Torino, 10129 Torino, Italy*
[*] *martin.blazek@physik.tu-darmstadt.de*

Abstract: Low coherent light interferometry requires broad bandwidth light sources to achieve high axial resolution. Here, Superluminescent Light Emitting Diodes (SLDs) utilizing Quantum Dot (QD) gain materials are promising devices as they unify large spectral bandwidths with sufficient power at desired emission wavelengths. However, frequently a dip occurs in the optical spectrum that translates into high side lobes in the coherence function thereby reducing axial resolution and image quality. We apply the experimental technique of frequency selective feedback to shape the optical spectrum of the QD-SLD, hence optimizing the coherence properties. For well-selected feedback parameters, a strong reduction of the parasitic side lobes by a factor of 3.5 was achieved accompanied by a power increase of 40% and an improvement of 10% in the coherence length. The experimental results are in excellent agreement with simulations that even indicate potential for further optimizations.

OCIS codes: (110.4500) Optical coherence tomography; (230.5590) Quantum-well, -wire and -dot devices; (230.7020) Traveling-wave devices

References and links

1. A. F. Fercher, W. Drexler, C. K. Hitzenberger, and T. Lasser, "Optical coherence tomography – principles and applications," Rep. Prog. Phys. **66**, 239-303 (2003).
2. D. C. Adler, Y. Chen, R. Huber, J. Schmitt, J. Connolly, and J. G.Fujimoto, "Three-dimensional endomicroscopy using optical coherence tomography," Nat. Photonics **1**, 709-716 (2007).
3. J. M. Schmitt, "Optical coherence tomography (OCT): A Review," IEEE J. Sel. Topics Quantum Electron. **4**, 1205-1215 (1999).
4. E. Alarousu, L. Krehut, T. Prykäri, and R. Myllylä, "Study on the use of optical coherence tomography in measurements of paper properties," Meas. Sci. Technol. **16** 1131–1137 (2005).
5. M. Grundmann, O. Stier, S. Bognar, and C. Ribbat, F.Heinrichsdorff, D.Bimberg, "Optical properties of self-organized quantum dots: Modeling and experiments," Phys. Stat. Sol.(A) **178**, 255-262 (2000).
6. M. Jedrzejewska-Szczerska, "Shaping coherence function of sources used in low-coherent measurement techniques," Eur. Phys. J. Special Top. **144**, 203–208 (2007).
7. M. Rossetti, L. Li, A.Markus, A. Fiore, L. Occhi, C. Vélez, S. Mikhrin, I. Krestnikov, and A. Kovsh, "Characterization and Modeling of Broad Spectrum InAs–GaAs Quantum-Dot Superluminescent Diodes Emitting at 1.2–1.3 µm," IEEE J. Quantum Electron. **43**, 676-686 (2007).
8. S. K. Ray, K. M. Groom, M. D. Beattie, H. Y. Liu, M. Hopkinson, and R. A. Hogg, "Broad-Band Superluminescent Light-Emitting Diodes Incorporating Quantum Dots in Compositionally Modulated Quantum Wells," IEEE Photon. Technol. Lett. **18**, 58-60 (2006).
9. Y. C. Xin, A. Martinez, T. Saiz, A. J. Moscho, Y. Li, T. A. Nilsen, A. L. Gray, and L. F. Lester, "1.3-µm Quantum-Dot Multisection Superluminescent Diodes With Extremely Broad Bandwidth," IEEE Photon. Technol. Lett. **19**, 501-503 (2007).
10. P. D. L. Judson, K. M. Groom, D. T. D. Childs, M. Hopkinson, and R. A. Hogg, "Multi-section quantum dot superluminescent diodes for spectral shape engineering," IET Optoelectron. **3**, 100-104 (2009).

#111898 - $15.00 USD Received 26 May 2009; revised 26 Jun 2009; accepted 26 Jun 2009; published 20 Jul 2009

11. M. Peil, I. Fischer, W. Elsäßer, S. Bakic, N. Damaschke, C. Tropea, S. Stry, and J. Sacher, "Rainbow refractometry with a tailored incoherent semiconductor laser source," Appl. Phys. Lett. **89**, 091106 (2006).
12. Y. Zhang, M. Sato, and N. Tanno, "Resolution improvement in optical coherence tomography by optimal synthesis of light-emitting diodes," Opt. Lett. **26**, 205-207 (2001).
13. A. C. Akcay, J. P. Rolland, and J. M. Eichenholz, "Spectral shaping to improve the point spread function in optical coherence tomography," Opt. Lett. **28**, 1921-1923 (2003).
14. D. S. Mamedov, V. V. Prokhorov, and S. D. Yakubovich, "Broadband radiation sources based on quantum-well superluminescent diodes emitting at 1550nm," Quantum Electron. **33**, 511-514 (2003).
15. P. Bardella, M. Rossetti, and I. Montrosset, "Modeling of Broadband Chirped Quantum-Dot Super-Luminescent Diodes," IEEE J. Sel. Topics Quantum Electron. **15**, 785-791 (2009).
16. E. V. Andreeva, M. V. Shramenko, and S. D.Yakubovich, "Double-pass superluminescent diode with tapered active channel," Quantum Electron. **32**, 112-114 (2002).
17. L. Mandel, "Fluctuations of Photon Beams: The Distribution of the Photo-Electrons," Proc. Phys. Soc. (London) **74**, 233-243 (1959).

1. Introduction

Over the past decade high resolution depth imaging has become a powerful diagnostic technique in medicine and surface analysis [1-4]. To achieve high axial resolution, light sources with a short coherence length are required. According to the Fourier transform theorem, a source with a broad-band, flat optical spectrum is necessary. Furthermore, each application defines a specific minimum output power at a preferred centre wavelength.

There are already light sources available, for example fibre-based or super continuum generating sources that meet most of the requirements. However, when integrability and cost efficiency become important, semiconductor light sources are superior. Especially superluminescent light emitting diodes (SLDs) based on Quantum Dot (QD) gain materials have raised much interest during the last years, as the emission properties can be tailored by the manipulation of the dot parameters [5]. The large spectral bandwidth arises from inhomogeneously broadened transitions of the QD ensemble. The transition with the lowest separation in energy is referred to as the ground state, followed by the first and higher excited states. Unfortunately, a dip occurs in the optical spectrum in between these transitions that introduces large side lobes in the coherence function and reduces the achievable resolution by the presence of ghost images [6]. In the past, several strategies as for example chirping of the QD layers [7] or compositionally modulating the embedding quantum wells [8] have been investigated to overcome the dip and realize ultra-broadband emission. However in each case, the fabricated devices did not fully meet the requirement of a broad and completely ripple-free emission spectrum with a high output power. Competing the recently presented multisection SLD [9, 10], we investigate post-technology methods to modify and optimize the coherence properties of fully processed devices [11]. In this letter, we present advances in the approach of spectral shaping [12-14] by the utilization of frequency selective feedback that proves to be a powerful, versatile optimization technique. By the introduction of suitable frequency selective elements inside the feedback branch, we can shape the optical spectrum thus optimizing the coherence properties accompanied by a power increase. We succeed to increase the output power by 40 percent, improve the coherence length by 10 percent and simultaneously suppress the side lobes by a factor of 3.5. The experimental results are in excellent agreement with simulations based on a spectrally resolved rate equation model described in [15] that even can give hints for further optimizations.

The paper is organized as follows. At first, the spectral distribution of the investigated QD-SLD is presented. Then, the experimental setup for frequency selective feedback and its implementation in the simulation is introduced, before the QD-SLD is further characterized without feedback. Exposed to feedback, the influence of the experimental parameters feedback strength and centre wavelength on the coherence properties of the SLD is discussed. For well-selected feedback parameters, the optimized coherence properties are presented along with simulation results. The achievements are summarized and strategies for exploitation of the method are sketched in the outlook.

#111898 - $15.00 USD Received 26 May 2009; revised 26 Jun 2009; accepted 26 Jun 2009; published 20 Jul 2009

2. Spectral Quantum Dot emission

The SLD under investigation consists of 6 identical InAs Quantum Dot layers embedded in InGaAs Quantum Wells. To avoid cavity effects the ridge waveguide is tilted by 7 degree with respect to the optical axis and a wide-band multi-layer anti-reflection coating is applied to both facets of the 6mm long device.

The optical spectrum of the QD-SLD emission is determined by the intensity distribution of the emitting QD transitions. Due to the carrier dynamics, the distribution and therefore the optical spectra depend on the pump current of the SLD. For low currents, the emission from the ground state (GS) transition is dominant (Fig. 1a), whereas for higher currents, the emission from the excited state (ES) transition becomes dominant (Fig. 1c). In between, at the equal power condition (EPC) point, both transitions emit equally intense (Fig. 1b). Here, the maximum spectral bandwidth is achieved and the most interesting operation regime for low coherent light interferometry is realized. Unfortunately, a dip occurs in the spectral region between ground and excited state emission. As a consequence of the pump current dependent optical spectra, the size of the dip also depends on the pump current. In Fig. 1a-c the vertical arrows schematically indicate the size of the dip. Shown in figure 1.d is the dip size for various pump currents of the investigated QD-SLD.

For low and high pump currents, in the GS or ES dominated regime, respectively, the dip exceeds 20dB. In between, the minimum value of 6dB is obtained at the equal power point at 362mA pump current. However, even the quite small dip of 6dB translates to rather high, parasitic side lobes in the coherence function and motivates the shaping of the optical spectrum by frequency selective feedback.

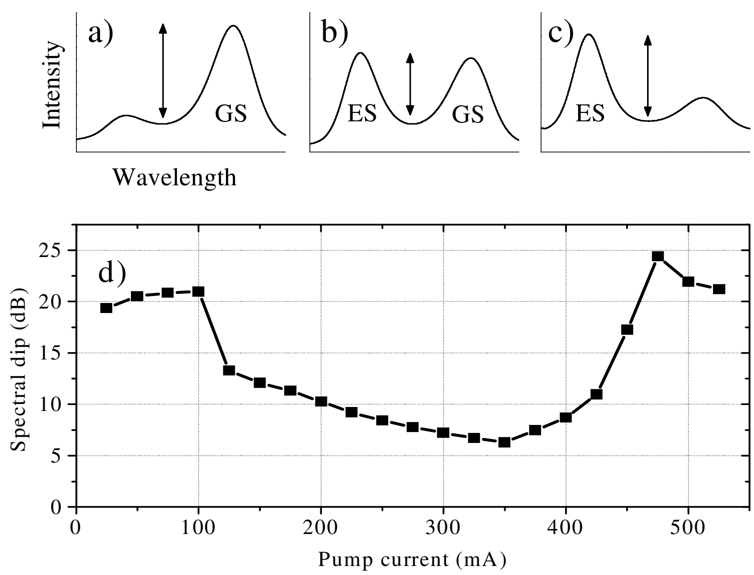

Fig. 1. Measured optical spectra of the investigated QD-SLD for various pump currents: (a) 225mA, (b) 362mA and (c) 425mA. The vertical arrows indicate the dip size. (d) Measured dip of QD-SLD.

3. Realization of frequency selective feedback:

The experimental setup for frequency selective feedback, illustrated in Fig.2, is based on a double pass configuration [14, 16]. The optical feedback is tailored from the SLD back facet emission. The collimated beam of the back facet passes a beam sampler (BS), an interference filter and a variable optical attenuator before being back reflected by a gold mirror. The beam sampler reflects a small amount of the emission and allows for back facet (P_{Back}) and feedback

#111898 - $15.00 USD Received 26 May 2009; revised 26 Jun 2009; accepted 26 Jun 2009; published 20 Jul 2009

power (P_{FB}) detection. The interference filter is chosen appropriately to fill the dip. The Gaussian transmission of the filter is centred at 1259nm with a full width at half maximum (FWHM) of 39nm. The centre wavelength of the feedback can be tuned to shorter wavelengths by tilting the filter and the feedback strength is adjusted by a variable optical attenuator. The back-reflected light is then injected into the SLD to optimize the front facet emission. The collimated beam of the front facet emission passes an optical isolator to avoid back reflections and a beam sampler to allow for measurement of the optical power (P_{Front}) before being focussed into a Fourier transform spectrometer to record the interferogram and reconstruct the optical spectrum via Fourier transformation.

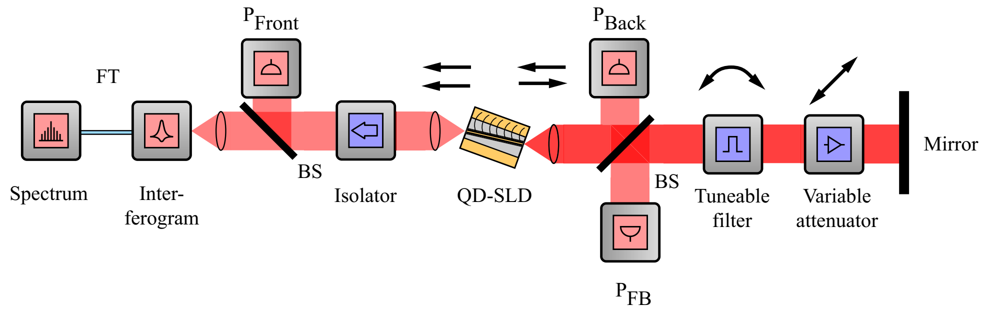

Fig. 2. Experimental realization of frequency selective feedback. In the centre the angle-tilted QD-SLD with bond wires is depicted.

4. Simulation of frequency selective feedback in QD SLDs:

Simulations are performed using the spectrally resolved rate equation model described in detail in reference [15]. The waveguide is properly discretized in its longitudinal direction in order to take into account spatial non-uniformity of gain and optical power. In each longitudinal section a set of rate equations is considered to compute the carrier distribution in the QD states and in the wetting layer. The QD band structure is supposed to consist of a two-fold degenerate GS and two upper exited states with degeneracy equal to 4 and 6 respectively; inhomogeneous broadening due to QD dot size dispersion is properly introduced in the calculation of gain and spontaneous emission rate. The main model parameters used in the simulations are listed in table 1.

Table 1. Main parameters used in the simulations.

QD emission wavelengths (ES_1,GS) [nm]	1220/ 1296	Electron relaxation times (Wetting layer→ES_2 / ES_2→ES_1 / ES_1→GS) [ns]	12/5.6 /12
Dot Density [μm^{-2}]	335	Wetting layer non- radiative recombination time [ns]	1.8
Maximum QD layer net gain (ES_1,GS) [cm^{-1}]	24.5/ 12.7	QD Auger recombination time [ps]	180
Internal losses [cm^{-1}]	2.4	QD inhomogeneous broadening width [meV]	55

#111898 - $15.00 USD Received 26 May 2009; revised 26 Jun 2009; accepted 26 Jun 2009; published 20 Jul 2009

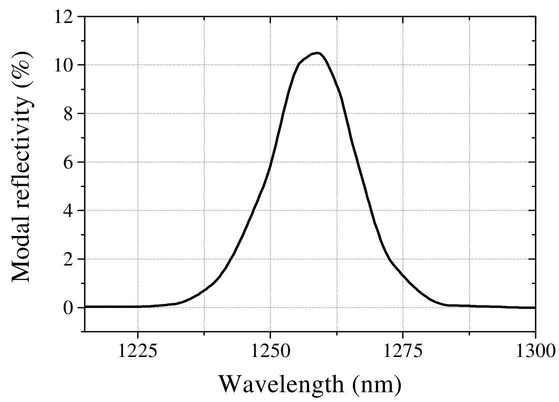

Fig. 3. Equivalent simulated modal reflectivity induced by the frequency selective optical feedback at the SLD back facet.

The frequency selective feedback is simply modelled as an additional wavelength dependent contribution to the modal reflectivity at the SLD back facet. Since the device facets are tilted and anti-reflection coated, the residual modal reflectivity without feedback at both facets is assumed to be 10^{-6} and wavelength independent. The additional contribution to the modal reflectivity due to the frequency selective feedback which allows a proper matching with the experiments has instead the bell shape behaviour shown in figure 3.

5. Experimental and modelling results:

At first, the QD-SLD without feedback is characterized. The measured SLD power-current characteristic in continuous-wave operation is shown together with the simulation results in figure 4.a). For low currents, the SLD emits spontaneously before amplified spontaneous emission (ASE) sets in at 300mA and the power increases significantly. This behaviour is well-reproduced in the simulation. Experimentally, the equal power condition (EPC) of GS and ES is realized at 362mA with an optical power of 1.5mW. In the simulation, the pump current for EPC is slightly smaller at 348mA. The inset shows the corresponding measured and simulated optical spectra at EPC. The centre wavelength of the GS emission is at 1296nm. The ES emission is centred at 1220nm. In between, at 1258nm a spectral dip of 6dB prevents the realization of a spectral bandwidth with 105nm FWHM. To investigate the influence of the dip on the coherence properties, the interferogram of the reference data without feedback was recorded to calculate the visibility $V = (I_{\mathbf{max}}-I_{\mathbf{min}})/ (I_{\mathbf{max}}+I_{\mathbf{min}})$ as shown in figure 4.b. In the simulation, the visibility is obtained by applying the inverse Fourier transform to the properly normalized optical power spectrum at the EPC. The modulation in the visibility due to the spectral dip is clearly visible by the presence of strong secondary coherence peaks at ±20µm. We define the contrast ratio C, by the ratio of the visibility between central to secondary coherence peak to characterize the height of the parasitic side lobes. The reference value $C_0 = 2.4$ is rather low and motivates the optimization of the coherence properties via spectral shaping.

Further characterization of the coherence properties is given by the coherence length $l_c = \int_{-\infty}^{\infty} |V(x)|^2 dx$ [17]. Without feedback, the coherence length of the SLD is $l_0 = 14.2$µm.

#111898 - $15.00 USD Received 26 May 2009; revised 26 Jun 2009; accepted 26 Jun 2009; published 20 Jul 2009

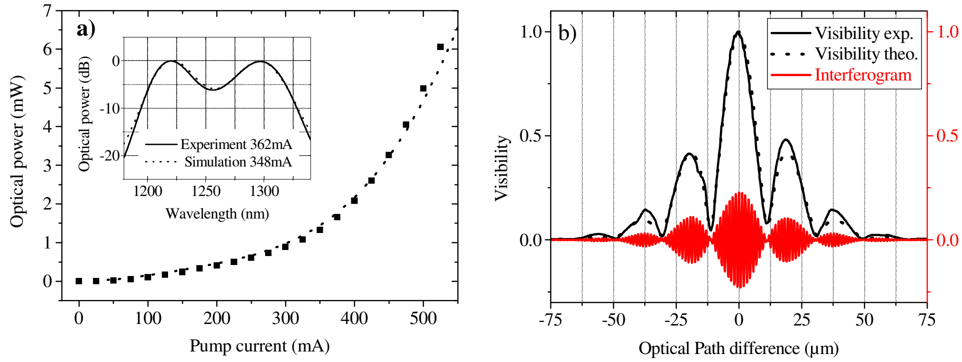

Fig. 4. QD-SLD characterization experiment **and** simulation (a) P-I-characteristic, inset: Optical spectra of investigated SLD at EPC, (b) Interferogram and visibility.

Optical feedback can initiate constructive or destructive effects on the coherence properties of semiconductor light sources [11]. QD-SLDs, as ASE sources, are sensitive to optical feedback. To optimize the coherence properties at the EPC, the dip has to be reduced by carefully adjusted frequency selective feedback. This was experimentally realized by the variation of centre wavelength and power of the feedback. The central transmission was tuned from 1249nm to 1259nm. The feedback power was varied from 0.33 to 2.0% of the unperturbed emission. To find the optimal setting, output power, coherence length and contrast ratio were measured.

The output power generally increases with the feedback strength. A map of relative increase in power is shown in figure 5.a) for various feedback settings. The increase in power is mainly independent of the feedback wavelength. Only for central wavelengths a small variation is observed. For 0.66% of feedback the power is raised by 30%, for 1% the power increases by 50% and even doubles for 2% of feedback. Considering only the increase in output power the use of large feedback strengths would seem favourable.

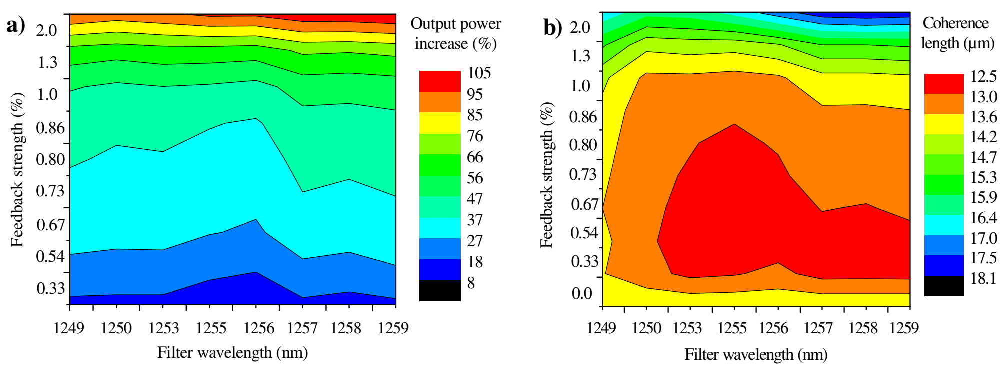

Fig. 5. Experimentally measured properties of QD-SLD for various feedback settings (a) relative power increase, (b) absolute coherence length with reference value (colour online).

On the contrary, the optimization of the coherence length disqualifies the use of large feedback strengths. The coherence length of the QD-SLD decreases when frequency selective feedback of moderate feedback strength is applied. For various feedback settings, the absolute values of the coherence length are shown in the map of coherence in figure 5.b). For moderate feedback strengths between 0.33 and 0.86% the coherence length is reduced below 13µm, corresponding to an improvement of 10% of the reference value l_0=14.2µm. For stronger feedback the coherence length increases as the spectral bandwidth is reduced. Again, a small wavelength dependence is observed for the central wavelength.

#111898 - $15.00 USD Received 26 May 2009; revised 26 Jun 2009; accepted 26 Jun 2009; published 20 Jul 2009

The side lobe suppression realized by frequency selective feedback is evident from the map of contrast shown in figure 6. In general, spectrally filtered feedback increases the contrast ratio. Compared to the reference value $C_0 = 2.4$, improvements by a factor of more than 3 are possible. To reduce the dip and therefore optimize the contrast ratio, careful adjustment of feedback power and centre wavelength is necessary. For medium feedback strengths the contrast ratio increases by a factor of at least 2. Fine tuning of the feedback wavelength maximizes the contrast in three islands with ratios above 8. There, the spectral position and the amount of feedback are properly set in relation to the SLD gain medium such, that the dip in between GS and ES emission is optimally filled.

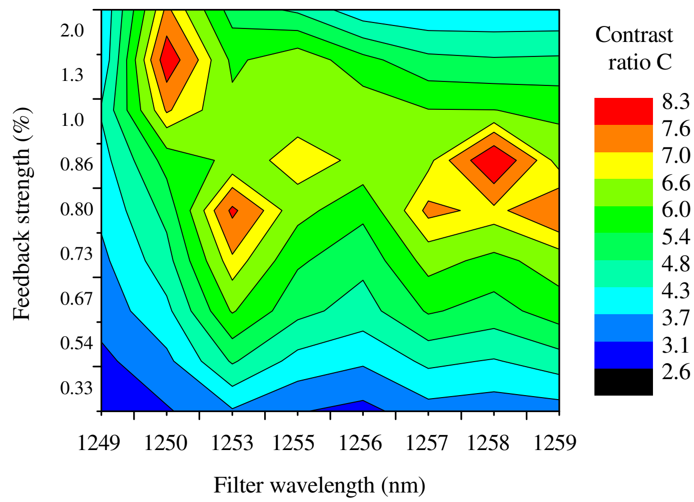

Fig. 6. Experimentally measured contrast ratio C of investigated QD-SLD for various FB settings (colour online).

The simultaneous optimization of the investigated parameters, especially regarding the contrast ratio, selects the optimal setting to 0.86% of feedback centred at 1258nm. Here, the output power increases by 43%, the coherence length is reduced by 10% to 12.9µm and the contrast ratio is successfully improved to 8.3. To confirm the experimental optimization of the coherence properties, the visibility and the optical spectrum with optimal feedback are compared to the simulation. The measured and simulated visibilities with optimal feedback and without feedback are shown in figure 7.a). With optimal feedback, the visibility of the side lobes is reduced by a factor of 3.5. This increases the contrast ratio of the coherence function and significantly improves the quality of OCT images.

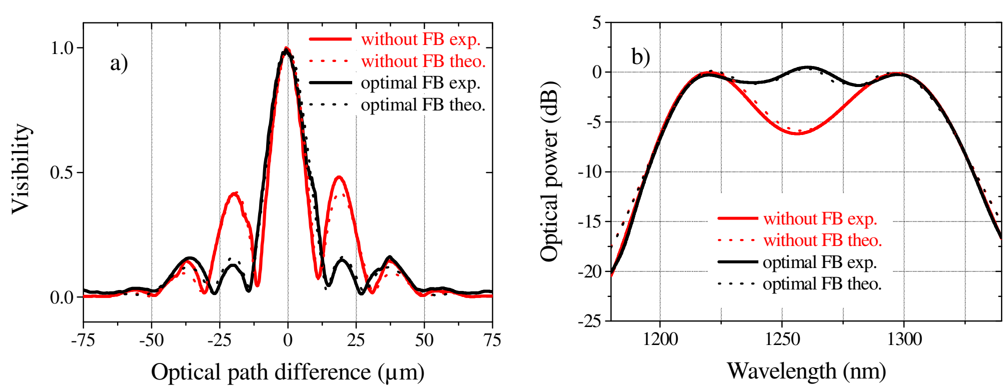

Fig. 7. Measured and simulated QD-SLD properties with optimal and without feedback: (a) Visibility, (b) Optical spectra.

#111898 - $15.00 USD Received 26 May 2009; revised 26 Jun 2009; accepted 26 Jun 2009; published 20 Jul 2009

The optimization of the coherence properties is a direct consequence of the reduced spectral dip. For comparison, the optical spectra of the SLD with optimal feedback and without feedback are shown in figure 7.b) together with simulation results. Obviously, the dip has been reduced by frequency selective feedback. An additional peak occurs in between GS and ES emission and reduces the spectral dip from 6dB to less than 1.8dB.

The improved optical spectrum implies, that in a future perspective, the simulations can be explored to find an ideal filter which fully reduces the dip at a given operation condition.

6. Conclusion and outlook

The coherence properties of a QD-SLD were optimized by frequency selective optical feedback. For well selected feedback parameters, the spectral dip in the emission spectrum between ground and excited state was minimized such, that the parasitic side lobes in the coherence function were suppressed by a factor of 3.5. Hence, the contrast ratio improved from 2.4 to 8.3 guaranteeing an ultrahigh resolution and ghost-free images in low coherent light interferometry. Simultaneously, the coherence length was reduced by 10% to 12.9µm accompanied by an increase in output power of 43%. With optimized feedback the investigated QD-SLD emitted 2.2mW of optical power with a spectral bandwidth of 105nm (FWHM) centred at 1260nm.

The experimental results demonstrate the impressive potential of frequency selective feedback. Compared to technological solutions, as for example chirping, frequency selective feedback is conceptually independent of wavelength and thereby guarantees a high degree of versatility. The presented experiments were carried out at the EPC of GS and ES emission. Nevertheless, in order to achieve higher output powers, the EPC of higher excited states could serve as a starting point for the feedback optimization. However, for higher pump currents the feedback sensitivity of the QD-SLD increases and care has to be taken to avoid the onset of laser action. Furthermore, the utilization of higher excited states shifts the central emission to shorter wavelengths. This shift is usually not desired by the application and has to be compensated for. One possible solution could involve the utilization of QD-SLDs with longer emission wavelengths that could still be optimized by frequency selective feedback. In principal, the technique is also device independent and can easily be adapted to other single pass ASE sources even QW-SLDs or fibre sources to realize nearly arbitrary spectral distributions by appropriate spectral filtering. The computational simulation, perfectly describing the experimental results, may guide towards design criteria for frequency selective elements. This becomes important, when the incorporation of the feedback technique into consumer-friendly SLD modules is considered. One possibility would be the simulation of a well-adapted coating on the surface of the module-integrated monitor photodiode, to generate a tailored frequency selective reflection. Another, probably more feasible realization scenario concerns the anti-reflection (AR) coating on the SLD facets that prevents lasing action in the solitary SLD. Here, the replacement of the AR coating on the back facet by a spectrally selective reflection coating could deliver the necessary filtered reflex.

Acknowledgments

This work has been performed within the Sixth Framework Programme EU STREP project Nano UB-Sources.

#111898 - $15.00 USD Received 26 May 2009; revised 26 Jun 2009; accepted 26 Jun 2009; published 20 Jul 2009